Jestr

Journal of Engineering Science and Technology Review 12 (3) (2019) 38 - 44

Research Article

JOURNAL OF
Engineering Science and Technology Review

www.jestr.org

Model Test of Influences of Pavement Static Loads on Reinforced Subgrade

Chen Guolong[1], Pang Chuanshan[2], Chen Fei[3], Ye Wanjun[4, 5], Cui Chenyang[4, 5*] and Yang Pengyu[6]

[1]*Hanzhong Highway Administration Bureau of Shaanxi Province, Hanzhong, Shaanxi Province, 723000, China*
[2]*Water Group Co., Ltd of Shaanxi Province, Xi'an, Shaanxi Province, 710068, China*
[3]*Chang'an University, Xi'an, Shaanxi Province, 710054, China*
[4]*College of Architectural and Civil Engineering of Xi'an University of Science and Technology, Xi'an, Shaanxi Province, 710054, China*
[5]*Road Engineering Research Center of Xi'an University of Science and Technology, Xi'an, Shaanxi Province, 710054, China*
[6]*Department of Civil, Geological and Mining Engineering, École Polytechnique de Montréal, Montreal H3C3A7, Canada*

Received 9 May 2019; Accepted 30 June 2019

Abstract

Reinforced subgrade has been increasingly used in highway and railway industries. Deformation failure of reinforced subgrade in the long-term operation has become a challenge against roadbed construction and maintenance. Static load of pavement is the key factor that influences stability of reinforced subgrade. The deformation law of reinforced subgrade and soil pressure distribution laws under staged static loads of pavement were analyzed by a laboratory large-scale model (4:1) test to reveal the influences of pavement static load on reinforced subgrade. Research results demonstrate that horizontal and vertical deformations of panel increase with static loads. Development loads of subgrade bearing capacity can slightly influence deformation after filler compaction, indicating that influences of static loads on subgrade deformation are closely related with the degree of filler compaction and rebar-soil interaction. Static loads of pavement considerably influence horizontal and vertical earth pressures at the subgrade top but slightly affect deep roadbeds. This outcome reflects that reinforcement accelerates attenuation of additional stress. The increased static loads of pavement slightly influence the strain state of subgrade geogrids. Distribution and value of geogrid strain in subgrade remain the same with the increase in static loads. This finding reveals that the formation of geogrid strain occurs during filling construction of subgrade. The compaction quality of filler can considerably influence the strain of geogrids. In summary, the influences of pavement static loads on reinforced subgrade are related to compaction quality during filling. Controlling the compaction degree of subgrade is the key to preventing deformation during the operational period. Research conclusions can provide theoretical references to control engineering diseases of reinforced subgrade and offer references to the construction of reinforced subgrade.

Keywords: Reinforced subgrade, Static load, Model test, Soil pressure, Deformation

1. Introduction

Reinforced subgrade is a structure comprising filler, reinforced materials, concrete facing, and connectors. Such a structure constrains deformation of fillers by "rebar-soil" interaction, thereby increasing the overall stability of subgrade [1]. In addition to the outstanding economic benefits, reinforced subgrade also has strong aseismic behavior [2]. Therefore, reinforced subgrade has been widely applied in subgrade construction engineering. However, reinforced subgrade develops various deformation failures, including longitudinal and transverse cracks, lateral deformation and vertical settlement of subgrade, and even local slump of the subgrade, in the long-term operation period. The Liandaowan Reinforced subgrade in Ansai Area has developed evident subsidence deformation of pavement, accompanied by certain bulging of the concrete facing and falling of partial concrete facing. The asphalt polystyrene board, which filled among settlement joints, has been extruded by approximately 2 cm. The Chagouping reinforced subgrade in Zichang County shows more serious deformation failures than those of Liandaowan Reinforced subgrade. The prefabricated concrete facings at two sides of the subgrade have developed evident bulges, and the maximum differential settlement of pavement has reached nearly 4 cm. Furthermore, the Baiyacun reinforced subgrade in Baota District was considerably destroyed by the strong rainfall for a long period in 2013, accompanied by large-scaled collapse of the subgrade. Reinforced materials are directly exposed to air, which may cause serious safety risks to traffic. Hence, deformation failure of reinforced subgrade during the operation is common.

The occurrence of the above-mentioned deformation failures is related to static loads of pavements undertaken by the reinforced subgrade during the operation period. Static loads mainly come from gravity of pavement structure, heaped loads of pavement, and traffic loads under low speed. Static loads of pavement increases the sliding force of the sliding soil wedge in the subgrade, which can deteriorate the stability of reinforced subgrade. The deformation problem of reinforced earth has attracted extensive research attention. Many field tests [3], laboratory tests [4-6], numerical simulations [7-8], and theoretical analyses [9-10] on deformation of reinforced subgrade have been reported. The mechanical properties of reinforced earth structure have been analyzed on the basis of these research methods,

*E-mail address: 1968047217@qq.com
ISSN: 1791-2377 © 2019 Eastern Macedonia and Thrace Institute of Technology. All rights reserved.
doi:10.25103/jestr.123.06

achieving satisfying results. These research conclusions are conducive to the comprehensive investigation of reinforced earth deformation. However, these studies mainly focus on the fracture surface state of reinforced subgrade or strength of reinforced earth mainly for optimization of design parameters. Only a few studies have discussed the deformation state of reinforced subgrade and distribution of soil pressure during the entire loading process of pavement. Therefore, a model test of reinforced subgrade under static loads of pavement is conducted by using the self-made loading system. This task is initiated to explore the influences of pavement static loads on deformation state and internal soil pressure distribution of reinforced subgrade. Results provide theoretical references to prevent diseases of reinforced subgrade engineering.

On this basis, the influences of pavement static loads on reinforced subgrade are discussed through a laboratory model test. These results laid foundations for quality assessment and maintenance program of reinforced subgrade during the operation period.

2. State of the art

Abundant theoretical and experimental studies on deformation behavior and characteristics of reinforced earth structure have been reported. A series of laws on deformation distribution of reinforced earth structure, earth pressure distribution, and strain distribution of reinforced materials can be concluded through a model test. Hence, a model test is widely applied in studies with complicated reinforced earth structures. Based on the basic experimental research results of Sharma model, a bearing capacity formula of foundation comprising reinforced sands and silty clay, which considerably conforms to model test results [11], is established. Through a centrifugal model test, Balakrishnan discussed influences of increased moisture content in backfill fine silt at subgrade edges on deformation failure of reinforced subgrade [12]. Alawaji conducted a static loading model test with variable positions of geogrid reinforcement and variable widths of materials. In this test, Alawaji concluded that the reinforcement efficiency was considerably increased with the geogrid width and decreased with depth [13]. Abu-Farsakh investigated the influences of the number of layers, interval, and tensile modulus of reinforced materials on the performance of reinforced sand foundation through a laboratory model test [14]. Fujita proposed a new maintenance method for reinforced subgrade, which had been used for several years, and verified the method by building a 6 m high laboratory model [15]. Based on model test and numerical simulation, Niroumand analyzed and evaluated the up-pull response of the symmetric anchoring plate with and without geogrid reinforcement layer by using the Plaxis software on the basis of model test and numerical simulation [16]. Mekonnen implemented a model test by using fly ash as filler and bamboo reinforcement as the reinforced material. He concluded that increasing the length and decreasing the lay interval of reinforced materials could relieve deformation of reinforced structures [17]. Ahmadi conducted a model test on the number of geotextile layers, interlayer vertical distance, and distance between the strip footing and the wall at the backfill top with and without reinforcements. He concluded that increasing the number of geotextile layers could considerably increase the ultimate bearing capacity and anti-deforming capability of the reinforced retaining wall [18]. Derksen implemented a laboratory model test to discuss bearing capacity of different reinforced retaining structures and then analyzed failure mechanism of reinforced retaining walls by using the digital image correlation method [19]. Furthermore, many scholars began to conduct model tests on reinforced earth structures under dynamic loading conditions [20-21]. Xiao studied the influences of basic position and loads of reinforced retaining wall on wall deformation under cyclic loads [22]. Liang performed a model test on a reinforced retaining wall with high iron content, finding small vertical settlement and horizontal deformation. The reinforced earth structure had good stability [23]. The existing studies are mainly experimental ones on construction technology of reinforced earth structure and selection of design parameters of retaining wall. With the increase in traffic flow, reinforced subgrade develops deformation failures pf different extents. The static loads of embankment made considerable contributions to changes in engineering quality of reinforced subgrade, which will be further studied. The influences of static loads of pavement on reinforced subgrade were investigated in this study. Moreover, the deformation law and soil pressure distribution law of reinforced subgrade under staged static loads of pavement were analyzed through a laboratory large-scaled model test.

The remainder of this study is organized as follows, Section 3 introduces the model test design and apparatus. Section 4 analyzes the model test. Section 5 summarizes the study conclusions.

3. Methodology

3.1 Model test apparatus

The mould case and loading system in this test used the multifunctional loading platform developed by Sanjin Electric Controlling Technology Co., Ltd of Shaanxi Province (Fig. 1). The loading system applied motor for loading, and the maximum loads could reach 3 × 104 kN. The loading speed was controlled with a frequency-controlled turbine reducer. The entire loading process was monitored by a sensor to assure accurate control of the static loading. The loading plate used 0.6 m (length) × 0.3 m (width) × 2 cm (height) iron plate to simulate the local static loads. The lower mould case was 2.2 m × 1.04 m × 1.8 m (length × width × height). The actual model size was 2.2 m × 1 m × 1.8 m according to the calculated similarity parameter equal to five, and the chamber height was slightly increased to assure test safety. The top and side of the mould case were free faces. The top was used for loading, and the side was utilized for panel construction. The side walls of the mould case comprised tempered glass, and the outer side was fixed by steel frame. Before the test, Vaseline was coated on four walls to reduce boundary effects. Bolts were used as the connector to assure plain strain state in the test process.

3.2 Selection of materials

Loess was collected from Huangling County, Yan´an City and used as fillers in the test. The relevant specifications [23] indicated that the basic physical properties of fillers were obtained from a basic mechanical test. The results are shown in Table 1, and the distribution of size is shown in Fig. 2.

Table 1. Basic physical properties of fillers

Index	Moisture content (%)	Optimal moisture content (%)	Liquid limit (%)	Plastic limit (%)	Proportion
Numerical value	5.6	16.5	31.2	21.5	2.72

Fig. 1. Loading test platform

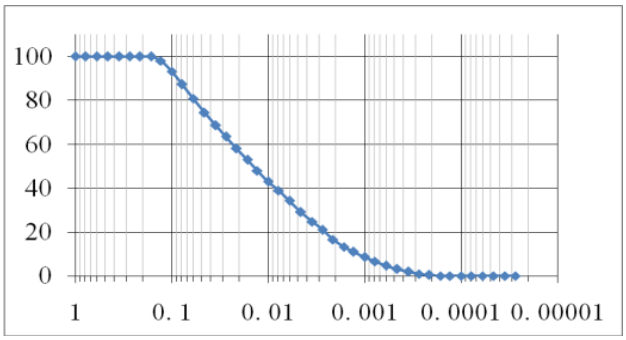

Fig. 2. Particle grading curve of Loess filler

Similarity theory indicated that the tensile modulus of reinforced materials in the model will be 1/5 of the prototype. Therefore, the TGDG35 one-way polypropylene geogrids were chosen as the reinforced material. The single rib width was 5.5 mm, and the thickness was 1 mm. The material parameters are listed in Table 2.

Table 2. Basic physical properties of geogrids

Index	Tensile strength (kN/m)	Tensile force at 2% elongation (kN/m)	Tensile force at 5% elongation (kN/m)
Numerical value	5.6	16.5	31.2

One end of geogrids was cast into the panel to assure hinge joint between reinforced materials and concrete facings. Hence, the degree of freedom of only one end of geogrids will be constrained.

3.3 Test scheme

Serious water loss was observed during filler transportation. Therefore, samples were wetted to make moisture content of filler close to the optimal moisture content. The compaction degree of subgrade was controlled by using a line scaling method. The sample mass of each layer was calculated according to relevant formulas. The degree of compaction can be considered satisfied when the samples are uniformly compacted to 15 cm thick.

In this test, soil pressure distribution and deformation must be monitored. The layout of the monitoring elements is shown in Fig. 3. The static loads were applied in stages in the test. The initial imposed stress was 10 kPa, and the loads were increased by 10 kPa in each stage until 60 kPa was reached. Data were read every 5 min under static loading. When the former and later readings were consistent, the reinforced subgrade reached stable deformation under this loading stage.

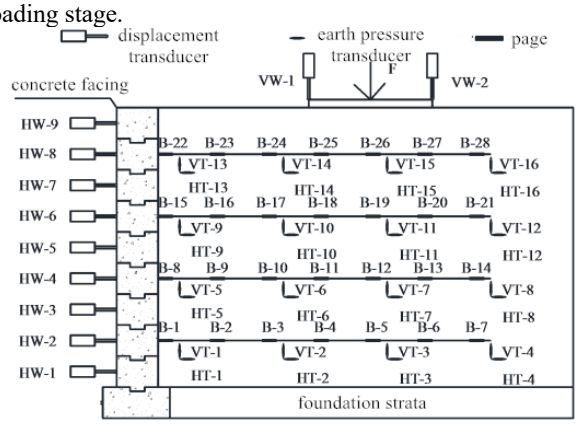

Fig. 3. Layout of monitoring elements

4. Result analysis and discussion

4.1 Horizontal deformation analysis of panel

Horizontal displacement of panels in different layers was tested with a linear displacement meter, and the results are shown in Fig. 4.

The figure shows that horizontal displacement at different heights varies with the increase in loads. The maximum horizontal displacement (0.28 mm) is achieved at the fifth panel. Meanwhile, the minimum displacement is achieved at the first panel (0.05 mm), which is only 0.02% of the subgrade height as manifested by evident bulge deformation. The deformation is slightly increased with the external loads, indicating the unremarkable increase in panel deformation. The analysis result of the relevant causes indicated that the degree of compaction and rebar-soil interaction increased with the gradual rising of external loads. Meanwhile, the ability of reinforced materials to restrict filler deformation is gradually developed, thus decreasing the follow-up horizontal deformation. The upper deformation of panels is larger than the lower one. This condition is attributed to the loading system that occupies the upper space of the mould case and the inadequate degree of compaction due to difficulties in compaction at the top.

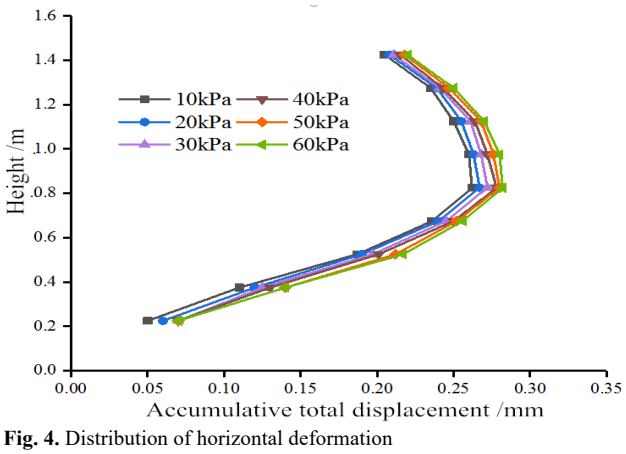

Fig. 4. Distribution of horizontal deformation

4.2 Vertical settlement at the top

The distribution law of vertical settlement at the top is shown in Fig. 5. The maximum vertical settlement is 3.6 mm at the end of loading, which is only 0.26% of the subgrade height. The external settlement of the loading plate is slightly higher than the internal one, which is approximately 0.3 mm. The development of vertical settlement can be divided into the following two stages 0-30 and 30-60 kPa. In the first stage, subgrade filler is in the compaction stage. However, the local degree of compaction is inadequate in the subgrade, and the rebar-soil interaction may be underused due to operational reasons for filling. Hence, vertical settlement rapidly develops and eventually reaches 2.6 mm, accounting for 79% of the final settlement. In the second stage, fillers are tightly arranged in subgrade. The fillers and geogrids are fully interacted, while the bearing capacity is completely developed, thus resulting in the small deformation (only 1.0 mm, 21% of the total settlement).

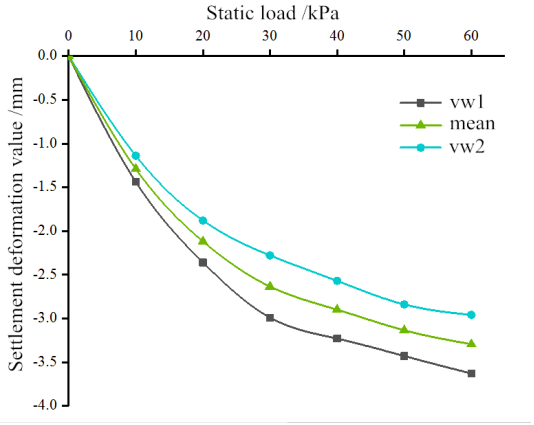

Fig. 5. Distribution of vertical settlement

4.3 Vertical earth pressure

The lowest layer is defined as the first layer. The monitored distribution of earth pressure in different layers is shown in Fig. 6.

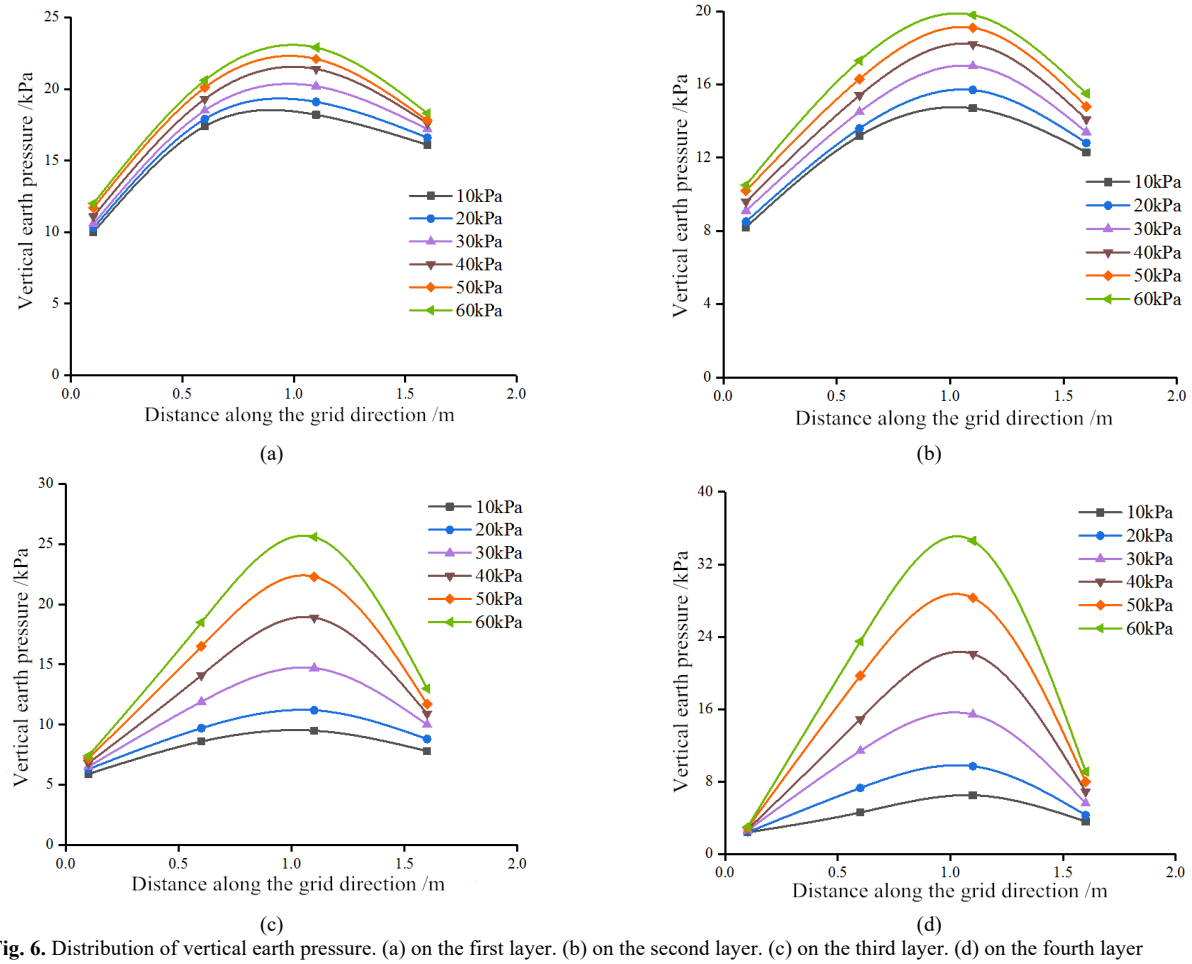

Fig. 6. Distribution of vertical earth pressure. (a) on the first layer. (b) on the second layer. (c) on the third layer. (d) on the fourth layer

As shown in Fig. 6, the distribution of vertical earth pressure is similar in different layers. The vertical earth pressure in different layers first increases and then decreases along the geogrids. The earth pressure peak occurs at the acting position of the loading plate, while the minimum one is at the position close to the panel. Such distribution is mainly caused by the following reason: the third sensor is below the loading plate and influenced by static loads. The minimum earth pressure close to the wall is attributed to the horizontal displacement of panel that releases partial earth pressure. Although earth pressure at different measuring points increases with the continuous increase of staged loads, vertical earth pressure at various positions makes distinct responses to external loads. The increased loads significantly affect vertical earth pressure in the third and fourth layers. However, such loads slightly influence the vertical earth pressure in the first and second layers. This finding reflects that a large area of fillers is accelerated after the

participation of soil reinforcement in the stress and attenuation of the additional stress. Notably, the vertical earth pressure is smaller than the traditional calculated results, indicating that reinforcement can decrease internal vertical earth pressure. This condition might be attributed to the supporting effect of reinforced materials, which weakens the transmission of vertical earth pressure.

4.4 Horizontal earth pressure

Curves were drawn according to data from vertically installed earth pressure sensors.

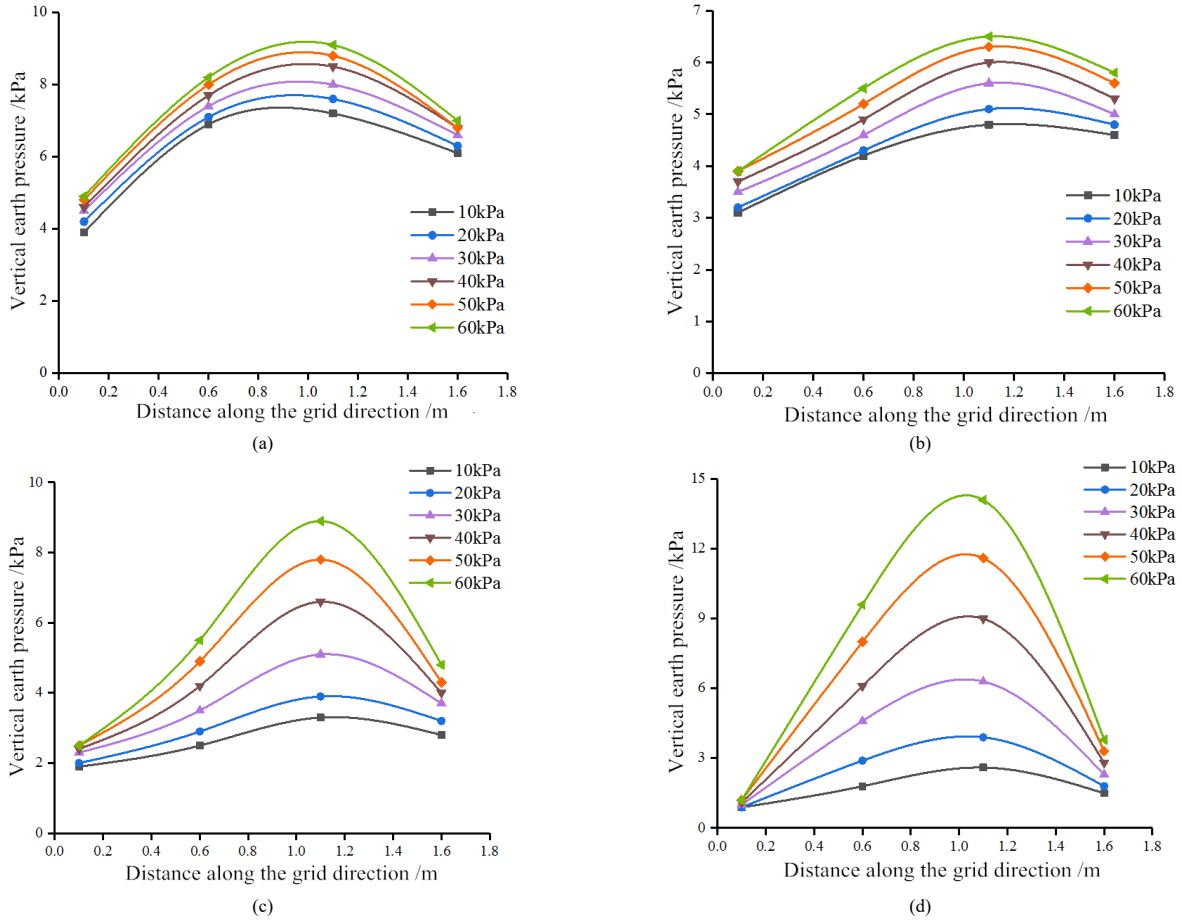

Fig. 7. Distribution of horizontal earth pressure. (a) on the first floor. (b) on the second floor. (c) on the third floor. (d) on the fourth floor

Similar to the distribution of vertical earth pressure, Fig. 7 shows the horizontal earth pressure first increases and then decreases along geogrids, reaching the peak at the middle point. The minimum peak is at one side close to the panel. The increase in external static loads mainly introduces the growth of earth pressure in the third and fourth layers. However, such an increase slightly affects the earth pressure in the first and second layers.

Notably, the theoretical maximum horizontal earth pressure is close to the panel. However, the maximum horizontal earth pressure is observed at the middle of geogrids in the test due to the following three reasons: (1) The additional stress diffuses due to the influence of the external static loads. (2) Horizontal displacement of the panel close to its side releases partial earth pressure. (3) The degree of compaction in the local regions close to the panel is inadequate due to structural characteristics of reinforced subgrade. This condition results in poor filler compaction and inadequate transmission of earth pressure.

4.5 Strain of geogrids

The strain distribution of geogrids in the staged application of static loads is shown in Fig. 8.

The figure shows that the strain of geogrids in the first three layers increases and then decreases along the geogrids. The strain of geogrids in the fourth layer shows the opposite variation law. The increased external static loads can slightly influence the strain of geogrids, and readings at certain measuring points remain constant. This finding indicates that the strain of geogrids is formed in the filling construction, and the external static loads can only slightly increase these strains. If the connection line of the maximum tensile strain is chosen as the potential slip surface, then the test results would differ with the conventional hypothesis of “0.3 H.” This outcome might be attributed to the uneven degree of compaction in the same layer and varying rebar-soil interaction due to the influences of soil arch. This phenomenon is considerably influenced by the degree of compaction control during construction and pavement quality of geogrids.

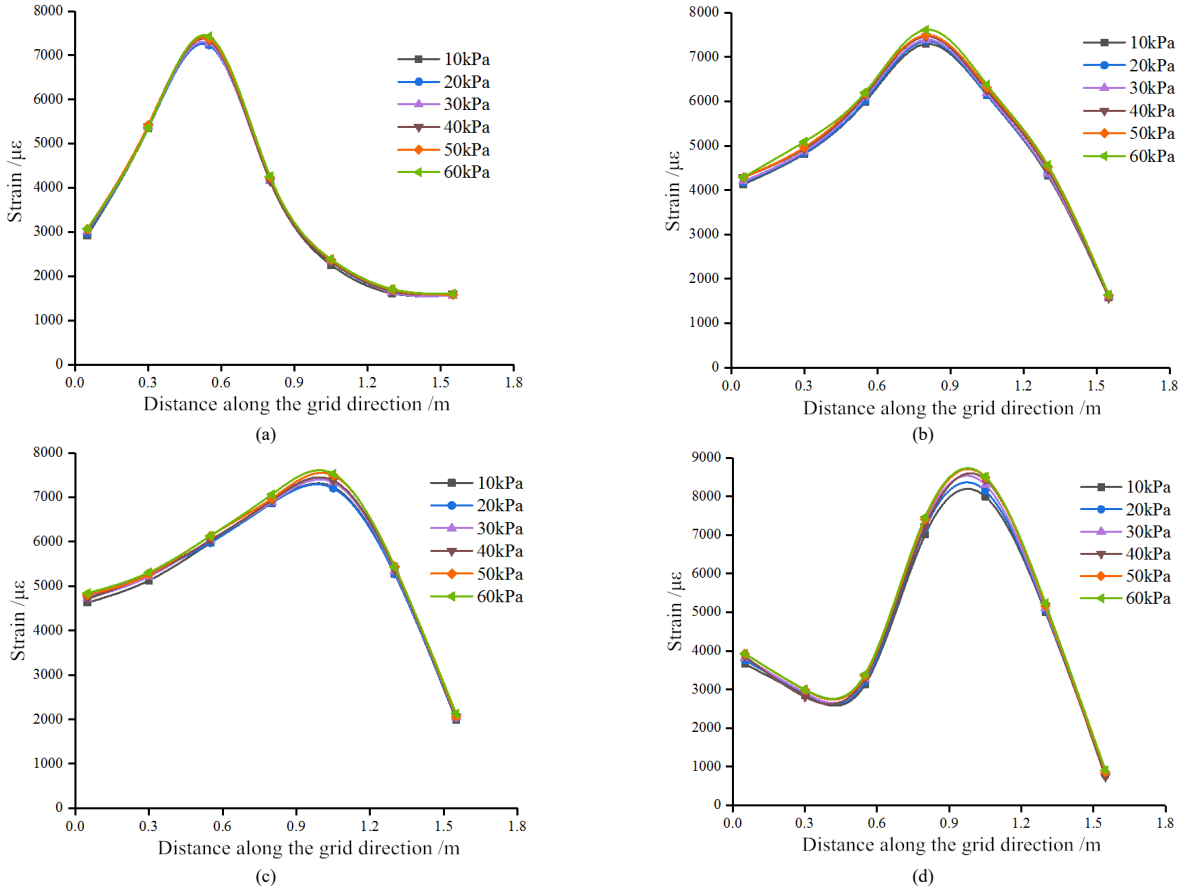

Fig. 8. Distribution of strain of geogrids. (a) in the first layer. (b) in the second layer. (c) in the third layer. (d) in the fourth layer

5. Conclusions

A model test of reinforced subgrade under staged static loads was conducted by using a self-made test system to reveal the effects of pavement static loads on deformation state and earth pressure distribution of reinforced subgrade. The laws of panel deformation, top settlement, earth pressure distribution, and deformation geogrids were analyzed. The following major conclusions could be drawn.

(1) Panel deformation of reinforced subgrade is mainly manifested as bulge characteristics under staged static loads. The maximum deformation (0.28 mm) is developed by the panel at the fifth layer. The increase in static loads slightly influences panel deformation.

(2) The maximum settlement deformation at the top of subgrade is 3.6 mm under the staged static loads. The settlement close to the wall is higher than that close to the midline. Deformation can be divided into two stages, namely, compaction and bearing capacity development. The degree of filler compaction plays an important role in vertical settlement.

(3) Vertical and horizontal earth pressures first increase and then decrease along the geogrids. The peaks of vertical and horizontal earth pressures are at the low section of the load source and the minimum ones are close to the wall. The increase in static loads considerably influences earth pressure in the third and fourth layers. However, such an increase slightly influences earth pressure in the first and second layers. The internal additional stress of reinforced subgrade rapidly attenuates.

(4) The increase in static loads can slightly influence the strain of geogrids. Such strain is mainly formed during the construction period. The respective compaction and pavement quality of fillers and geogrids considerably influence distribution of geogrid strains.

In summary, the influences of pavement static loads on reinforced subgrade are discussed through a model test. The similarity parameter value is reasonable, and the model materials are accurately selected, thus obtaining simple and explicit laws. The research results can effectively reflect deformation distribution and earth pressure distribution laws of reinforced subgrade under static loads of pavement. Other research results concerning influences of pavement static loads on reinforced subgrade have been achieved. However, the influences of pavement static loads on reinforced subgrade are unrelated to the influencing position. In this study, the static loads acting on the middle of roads under common conditions are discussed without considering the situation when pavement loads are at one side of the subgrade. Therefore, research results have a certain error with practical situation. Future systematic studies of the influences of pavement static loads on reinforced subgrade with considerations to different acting positions of loads are needed

This is an Open Access article distributed under the terms of the Creative Commons Attribution License

References

1. Skinner, G. D., Rowe, R. K., "Design and behaviour of a geosynthetic reinforced retaining wall and bridge abutment on a yielding foundation". *Geotextiles & Geomembranes*, 23(3), 2005, pp.234-260.
2. Anastasopoulos, I., Georgarakos, T., Georgiannou, V, et al., "Seismic performance of bar-mat reinforced-soil retaining wall: Shaking table testing versus numerical analysis with modified kinematic hardening constitutive model". *Soil Dynamics and Earthquake Engineering*, 30(10), 2010, pp.1089-1105.
3. Desai, C, S., Elhoseiny, K. E., "Prediction of reinforced soil wall using advanced constitutive mode". *Journal of Geotechnical and Geoenvironmental Engineering*, 133(1), 2005, pp.729-739.
4. Suzuki, M., Nakashita, A., Tsukuda, K., et al., "Applicability of clinker ash as fill material in steel strip-reinforced soil walls". *Soils and Foundations*, 58(1), 2018, pp.16-33.
5. Eigenbrod, K. D., Locker, J. G., "Determination of friction values for the design of side slope slined or protected with geosynthetics". *Canadian Geotechnical Journal*, 24(4), 1987, pp.509-519.
6. Alrefeai, T. O., "Behavior of granular soils reinforced with discrete randomly oriented inclusions". *Geotextiles and Geomembranes*, 10(4), 1991, pp.319-333.
7. Feng, S. L., Li, J., Li, P. L., "Numerical Evaluation of the Active Earth Pressure Acting on Rigid Retaining Walls". *Applied Mechanics and Materials*, 204-208, 2012, pp.410-413.
8. Senthil, K., Iqbal, M. A., Kumar, A., "Behavior of cantilever and counterfort retaining walls subjected to lateral earth pressure". *International Journal of Geotechnical Engineering*, 8(2), 2014, pp.167-181.
9. Sawicki, A., Kulczykowski, M., "Pre-failure behaviour of reinforced soil". *Geotextiles & Geomembranes*, 13(4), 1994, pp.213-230.
10. Ensan, M. N., Shahrour, I., "A macroscopic constitutive law for elasto-plastic multilayered materials with imperfect interfaces: Application to reinforced soils". *Computers & Geotechnics*, 30(4), 2003, pp.339-345.
11. Sharma, R., Chen, Q., Abu-Farsakh, M., et al., "Analytical modeling of geogrid reinforced soil foundation". *Geotextiles and Geomembranes*, 27(1), 2009, pp.63-72.
12. Balakrishnan, S., Viswanadham, B. V. S., "Performance evaluation of geogrid reinforced soil walls with marginal backfills through centrifuge model tests". *Geotextiles & Geomembranes*, 44(1), 2016, pp.95-108.
13. Alawaji, H. A., "Settlement and bearing capacity of geogrid-reinforced sand over collapsible soil". *Geotextiles & Geomembranes*, 19(2), 2001, pp.75-88.
14. Abu-Farsakh, M., Chen, Q., Sharma, R., "An experimental evaluation of the behavior of footings on geosynthetic-reinforced sand". *Soils and Foundations*, 53(2), 2013, pp.335-348.
15. Fujita, T., Kubo, T., Miyatake, H., et al., "A full scale model test of geogrid reinforced soil wall for establishment of it´s maintenance method". *Perspective Papers*, 29, 2014, pp.155-160.
16. Niroumand, H., Kassim, K. A., "Uplift response of symmetrical anchor plates in reinforced cohesionless soil". *Arabian Journal of Geosciences*, 7(9), 2014, pp.3755-3766.
17. Mekonnen, A. W., Mandal, J. N., "Behaviour of Bamboo–Geogrid Reinforced Fly Ash Wall Under Applied Strip Load". *International Journal of Geosynthetics and Ground Engineering*, 3(3), 2017, pp.24.
18. Ahmadi, H., Hajialilue-Bonab, M., "Experimental and analytical investigations on bearing capacity of strip footing in reinforced sand backfills and flexible retaining wall". *Acta Geotechnica*, 7(4), 2012, pp.357-373.
19. Derksen, J., Ziegler, M., Detert, O., et al., "Ground breaking events for geogrid -reinforced support structures". *Bautechnik*, 94(9), 2017, pp.656-660.
20. Lin, Y. L., Yang, G. L., Li, Y., et al., "Test study on dynamic deformation behavior of reinforced gabion retaining wall under cyclic load". *Chinese Journal of Rock Mechanics and Engineering*, 28(S2), 2009, pp.4027-4033.
21. Liu, Z., Shi, K. Y., Lei, Y., "Model test on dynamic characteristics of geogrid reinforced earth retaining wall packet ecological bag under repeated loading". *Journal of Vibration and Shock*, 34(9), 2015, pp.88–94.
22. Xiao, C. Z., Wang, J. Y., Zhou, X., "Performance study of geogrid-reinforced soil retaining walls subjected to static and cyclic footing loading". *Chinese journal of rock mechanics and engineering*, 36(06), 2017, pp.1542-1550.
23. Liang, X. Y., Jin, J., Yang, G. Q., "Experimental Study on Geogrid Reinforced Earth Retaining Wall of High Speed Railway". *Railway Engineering*, 2017(7), 2017, pp.108-111.
24. GBT50123-1999., "*standard for soil test method*". Beijing: China Planning Press, China, 1999.